Mathematical Biosciences and Engineering

MBE, 20(6): 10339–10357.
DOI: 10.3934/mbe.2023453
Received: 09 December 2022
Revised: 16 February 2023
Accepted: 28 February 2023
Published: 31 March 2023

http://www.aimspress.com/journal/MBE

Research article

Development and validation of two redox-related genes associated with prognosis and immune microenvironment in endometrial carcinoma

Yan He[1,2,†], Nannan Cao[2,†], Yanan Tian[1,2], Xuelin Wang[2], Qiaohong Xiao[2], Xiaojuan Tang[3], Jiaolong Huang[2], Tingting Zhu[2], Chunhui Hu[4], Ying Zhang[5], Jie Deng[2], Han Yu[2,6,*] and Peng Duan[2,*]

[1] Postgraduate Union Training Base of Jinzhou Medical University, Xiangyang No.1 People's Hospital, Hubei University of Medicine, Xiangyang 441000, China
[2] Affiliation Key Laboratory of Zebrafish Modeling and Drug Screening for Human Diseases of Xiangyang City, Department of Obstetrics and Gynaecology, Xiangyang No. 1 People's Hospital, Hubei University of Medicine, Xiangyang 441000, China
[3] Department of Radiography center, Renmin Hospital, Hubei University of Medicine, Shiyan 442000, China
[4] Department of Clinical Laboratory, Xiangyang No.1 People's Hospital, Hubei University of Medicine, Xiangyang 441000, China
[5] Laboratory of Medical Genetics, Harbin Medical University, Harbin 150000, China
[6] Department of Pathology, Xiangyang No.1 People's Hospital, Hubei University of Medicine, Xiangyang 441000, China

* **Correspondence:** Email: yuhanqh@163.com, meduanpeng@163.com.

† These two authors contributed equally.

Abstract: In recent studies, the tumourigenesis and development of endometrial carcinoma (EC) have been correlated significantly with redox. We aimed to develop and validate a redox-related prognostic model of patients with EC to predict the prognosis and the efficacy of immunotherapy. We downloaded gene expression profiles and clinical information of patients with EC from the Cancer Genome Atlas (TCGA) and the Gene Ontology (GO) dataset. We identified two key differentially expressed redox genes (*CYBA* and *SMPD3*) by univariate Cox regression and utilised them to calculate the risk score of all samples. Based on the median of risk scores, we composed low-and high-risk groups and

performed correlation analysis with immune cell infiltration and immune checkpoints. Finally, we constructed a nomogram of the prognostic model based on clinical factors and the risk score. We verified the predictive performance using receiver operating characteristic (ROC) and calibration curves. *CYBA* and *SMPD3* were significantly related to the prognosis of patients with EC and used to construct a risk model. There were significant differences in survival, immune cell infiltration and immune checkpoints between the low-and high-risk groups. The nomogram developed with clinical indicators and the risk scores was effective in predicting the prognosis of patients with EC. In this study, a prognostic model constructed based on two redox-related genes (*CYBA* and *SMPD3*) were proved to be independent prognostic factors of EC and associated with tumour immune microenvironment. The redox signature genes have the potential to predict the prognosis and the immunotherapy efficacy of patients with EC.

Keywords: endometrial carcinoma; redox; immune microenvironment; prognosis; bioinformatics

1. Introduction

Endometrial carcinoma (EC) is one of the three major gynaecological tumours in the world, and its incidence has increased [1]. The incidence of EC is higher than cervical cancer, and the mortality is higher than cervical cancer and ovarian cancer [2]. EC accounts for 76,000 deaths among women each year worldwide [3]. Currently, the main treatments for EC are surgery, radiotherapy, and chemotherapy. In recent years, with the development of clinical research, immunotherapy has shown good efficacy in patients with EC [4]. However, some patients have a poor response to immunotherapy [5]. Thus, it is urgent to find new biomarkers to predict the prognosis of patients with EC to facilitate better treatment stratification and to improve the survival.

Redox homeostasis plays an important role in biological processes, including cell growth, proapoptotic, impaired phagocytosis, ferroptosis, cell migration, and invasion, among others [6–13]. Recent studies have highlighted that redox homeostasis imbalance is related to immune system diseases and tumours [14–15]. Additionally, researchers have developed many prognostic models with redox-related genes to predict the prognosis or death risk of patients with various tumours [16–19]. In EC Ishikawa cells, an abnormal redox state inhibited cell migration and invasion and induced cell death by ferroptosis [20]. Although redox is strongly associated with EC, few studies have shown that redox-related biomarkers could improve the prognostic prediction of patients with EC.

In the present study, we identified and verified a redox-related prognostic signature to predict the prognosis of patients with EC, whose information was downloaded from The Cancer Genome Atlas Uterine Corpus Endometrial Carcinoma (TCGA-UCEC). Their differential expression resulted in different survival rates and responses to immunotherapy. This prognostic model constructed from the two molecules might provide instructions for predicting prognosis and assessing the effectiveness of immunotherapy for patients with EC.

2. Materials and methods

2.1. Collection of gene expression profiles

The gene expression profiles of 583 samples (548 EC samples and 35 paracancerous samples) were downloaded from TCGA (https://portal.gdc.cancer.gov/repository). Among the 548 patients with EC, 544 with complete survival and clinical information, including age at initial diagnosis, grade, stage, status, and histological type of tumour, were selected for the construction and validation of the risk model. Meanwhile, 55 redox genes were screened by searching redox-related gene annotations in the Gene Ontology (GO) database (http://geneontology.org/). The retrieved gene annotation terms included 'GO_CELL_REDOX_HOMEOSTASIS', 'GO_RESPONSE_TO_REDOX_STATE', 'GO_CELLULAR_RESPONSE_TO_REDOX_STATE', 'GO_DETECTION_OF_REDOX_STATA' and 'GO_REDOX_TAXIS'.

2.2. Identification of redox-related differentially expressed genes (DEGs)

The R package 'DESeq2' (version 1.32.0) was used to recognize the DEGs between tumour and paracancerous samples. $|\log2\ FC| > 1$ and $P_{adj} < 0.05$ were considered to be statistically significant. In total, 8593 DEGs (including 2962 downregulated genes and 5631 upregulated genes) were screened out. Meanwhile, 14 redox-related DEGs were extracted by considering the intersection between redox genes and DEGs.

2.3. Go and kyoto encyclopedia of genes and genomes (KEGG) enrichment analysis

Fourteen redox-related DEGs were selected for enrichment analysis to reflect the biological functions of these genes in patients with EC by using the R package 'ClusterProfiler' (version 4.0.5). Enrichment analysis referred to cellular components, molecular functions, biological processes and signalling pathways. The function "enrichGO" and "enrichKEGG" were applied, respectively. P_{adj} values < 0.05 were considered significantly different.

2.4. Construction and verification of redox-related gene risk model

Two prognostic redox-related DEGs (cytochrome *b*-245 alpha chain [*CYBA*] and sphingomyelin phosphodiesterase 3 [*SMPD3*]) were screened out from the 14 redox-related DEGs by using univariable Cox regression analysis with $P_{adj} < 0.05$. A hazard ratio (HR) < 1 was a protective factor and conversely, an HR ≥ 1 was a risk factor. *CYBA* and *SMPD3* were used to construct a risk model. The formula for the risk score of each sample was calculated as follow: Risk Score = (-0.2190351 × *CYBA*) – (0.3898170 × *SMPD3*). The study selected 544 patients with EC with complete survival information and gene expression profiles in the TCGA-UCEC dataset. Then, they were randomly divided into a training set (381 patients) and a test set (163 patients) based on a 7:3 ratio. Based on the median risk score, patients were divided into low-and high-risk groups in the training and test sets. Kaplan-Meier (KM) survival curves were plotted by using the R package 'survival' (version 0.4.9) to compare the overall survival (OS) between the two subgroups, and time-dependent receiver operating characteristic (ROC) curves were plotted with area under the curve (AUC) to assess the accuracy of

the model in predicting prognosis.

2.5. Immunohistochemistry (IHC) staining

We estimated the protein expression levels of CYBA and SMPD3 paracancerous and tumour tissue by IHC staining. The endometrial tissues from health and patients of EC were fixed in 4% neutral formalin, embedded in paraffin, sliced (4 μm), and then subjected to IHC staining. After dewaxed in xylene two times, hydrated in gradient ethanol five times, and antigen retrieval at 37℃, the slides were incubated with rabbit anti-CYBA or anti-SMPD3 primary antibodies (dilution 1:300, Bioss, bs-3879R, and bs-11193R) at 4℃ overnight.The following day, the slides were incubated with secondary antibody. We observed and obtained the digital images of the stained tissue slides at ×20 and ×40 magnification with an optical microscope.

2.6. Gene set variation analysis (GSVA) of low-and high-risk groups

We further explored the differences in biological processes between the low-and high-risk groups. The gsva function of the R package 'GSVA' (version 1.40.1) with the default value was applied to perform GSVA for each sample [21]. The gene sets of the low-and high-risk groups were sourced from the R package 'msigdbr' (version 7.4.1).

2.7. Estimation of immune cell infiltration fractions

The R package 'IOBR' was used to determine the difference in immune cell infiltration calculated by using the xCell algorithm in the low-and high-risk groups [22]. The immune score and stromal score were calculated using the R package 'ESTIMATE' (version 1.0.13) to determine the Spearman correlation coefficients between the risk score and the estimation score, including the stromal score and the immune score for each EC sample.

2.8. Mutation analysis

The mutation information of patients with EC was downloaded from the TCGA-UCEC database. Meanwhile, the mutation data of somatic variants were extracted from Mutation Annotation Format (MAF). The R package 'maftools' was utilised to perform Fisher's exact test for the mutation data of somatic variants between the low-and high-risk groups. First, the top 20 genes with somatic mutations were visualised in the low-and high-risk groups to compare the tumour mutation burden. Then, a summary of all mutation types was visualised in the TCGA-UCEC cohort.

2.9. Construction and validation of the nomograms

Univariate and multivariate Cox analyses were performed to assess whether the risk model and clinical features could be deemed independent prognostic factors of patients with EC. The R package 'rms' was utilised to construct a nomogram to predict 3-, 5- and 7-year survival rates of patients with EC. KM, ROC and calibration curves of 3-, 5- and 7-year were used to evaluate the accuracy of the nomogram.

2.10. Statistical analysis

All data analysis was conducted with R software (version 4.0.5, http://www.r-project.org), including the following packages: clusterProfiler, DESeq2, estimate, GEOquery, ggplot2, ggrepel, ggstatsplot, GOplot, GSVA, IOBR, magrittr, msigdbr, pheatmap, pROC, reshape2, rms, stringr, survival, survminer and VennDiagram. The Wilcoxon test was performed to analyse differences between the two groups and Spearman rank correlation was applied to test the correlation between the two groups. Samples with $P < 0.05$ were considered statistically significant.

3. Results

3.1. Identification of redox genes in patients with EC

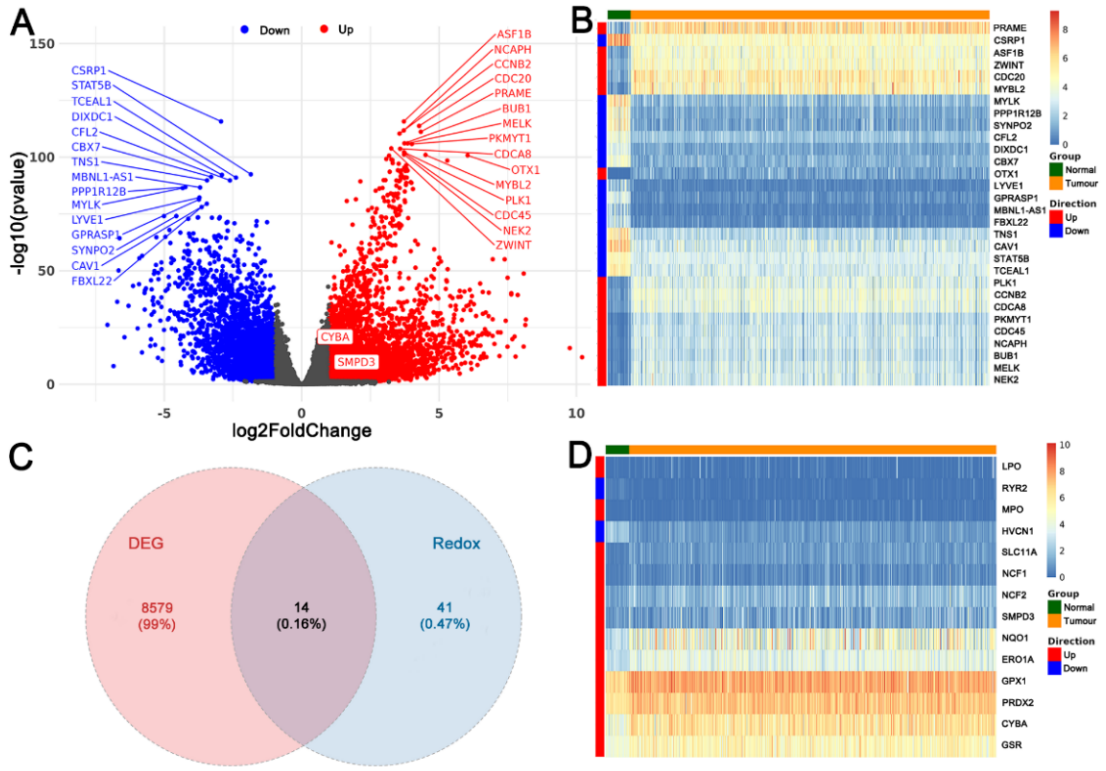

Figure 1. Expresssion of redox-related DEGs in paracancer and tumour tissues. (A) Volcano plot of the DEGs in paracancer and tumour tissues. Red indicates up-regulated gene, blue indicates down-regulated gene. (B) Heatmap of DEGs in paracancer and tumour tissue. (C) Venn diagram of redox-related DEGs in paracancer and tumour tissue. (D) Heatmap of redox-related DEGs in paracancer and tumour tissue.

The flow chart of our study design is shown in Figure S1. The DEGs were extracted by comparing the expression level in paracancerous and tumour samples ($|\log2FC| > 1$, $P_{adj} < 0.05$) from TCGA-UCEC data (Figure 1A). We obtained 8593 DEGs through the R package 'DESeq2', including 2962 upregulated genes and 5631 downregulated genes. Figure 1B shows the top 15 up- and down-regulated DEGs in paracancerous and tumour tissues. Then, we selected the redox genes among the DEGs. As

the Venn diagram shows, we identified 14 candidate genes as the redox-related DEGs of patients with EC (Figure 1C). Figure 1D shows significant differential expression of the 14 candidate genes of EC in paracancerous and tumour samples.

3.2. Functional annotation of redox-related DEGs

We performed GO term and KEGG pathway enrichment analysis of the 14 candidate redox-related genes. GO enrichment analysis showed that these genes were mainly enriched in cell redox homeostasis, response to oxidative stress, and cellular response to chemical stress in the biological process (Figure 2A). These genes were mainly involved in antioxidant activity, oxidoreductase activity, and acting on NAD(P)H and electron transport in the molecular function (Figure 2B). These genes were mainly located in endocytic vesicle, secretory granule membrane, and oxidoreductase complex in the cellular component (Figure 2C). Meanwhile, the KEGG pathway analysis showed the 14 candidate genes were significantly enriched in 12 pathways (Figure 2D). These pathways, including chemical carcinogenesis-reactive oxygen species, neutrophil extracellular trap formation, leucocyte transendothelial migration, and glutathione metabolism, are potentially related to the occurrence of EC.

3.3. A prognostic signature based on redox-related DEGs

We randomly divided the 544 patients in the TCGA group into a training set (381 patients) and a test set (163 patients) in a 7:3 ratio. We used the training set to construct a prognostic risk signature, and we used the test set to validate the risk score model. Based on the training set, we employed univariate Cox regression to identify prognostic DEGs among the 14 candidate genes with the threshold value of $P < 0.05$. Finally, we identified two prognostic hub genes – *CYBA* and *SPMD3* – that could serve as protective factors (HR < 1) for patients with EC (Figure 3A). In IHC staining, CYBA and SMPD3 protein expression increased in EC tissue more than in paracancerous tissue (Figure 3B). Figure S2 showed that signal pathways and GO terms involved in *CYBA* and *SMPD3* in tumour diseases. *CYBA* enriched in "neutrophil mediated immunity", "neutrophil activation" and "NRF2-KEAP1 and PIK3 signaling pathway". *SMPD3* enriched in "colorectal cancer metastasis signaling", "foxO signaling pathway" and "metabolic pathways".

To evaluate the prognostic value of the two redox-related genes, we used the training and test sets concurrently. Based on the risk model, we calculated and ranked the risk scores of patients with EC in the training sets. Each patient is marked by a dot and their survival status is marked on the dot plot to display distribution (Figure 4A). Meanwhile, according to the median risk score, we classified patients into low-and high-risk groups. The distribution of survival status and risk score for patients with EC was shown in Figure 4B. The survival status of patients in the test sets is the same as that in the training sets (Figure 4C,D). KM survival analysis showed the OS of patients in the low-risk group was significantly longer than those in the high-risk group (Figure 4E). Besides, the 3-, 5- and 7-year AUC of ROC curves in the training sets were 0.647, 0.724, and 0.692, respectively (Figure 4F), which are similar to that in the test sets (Figure 4G,H).

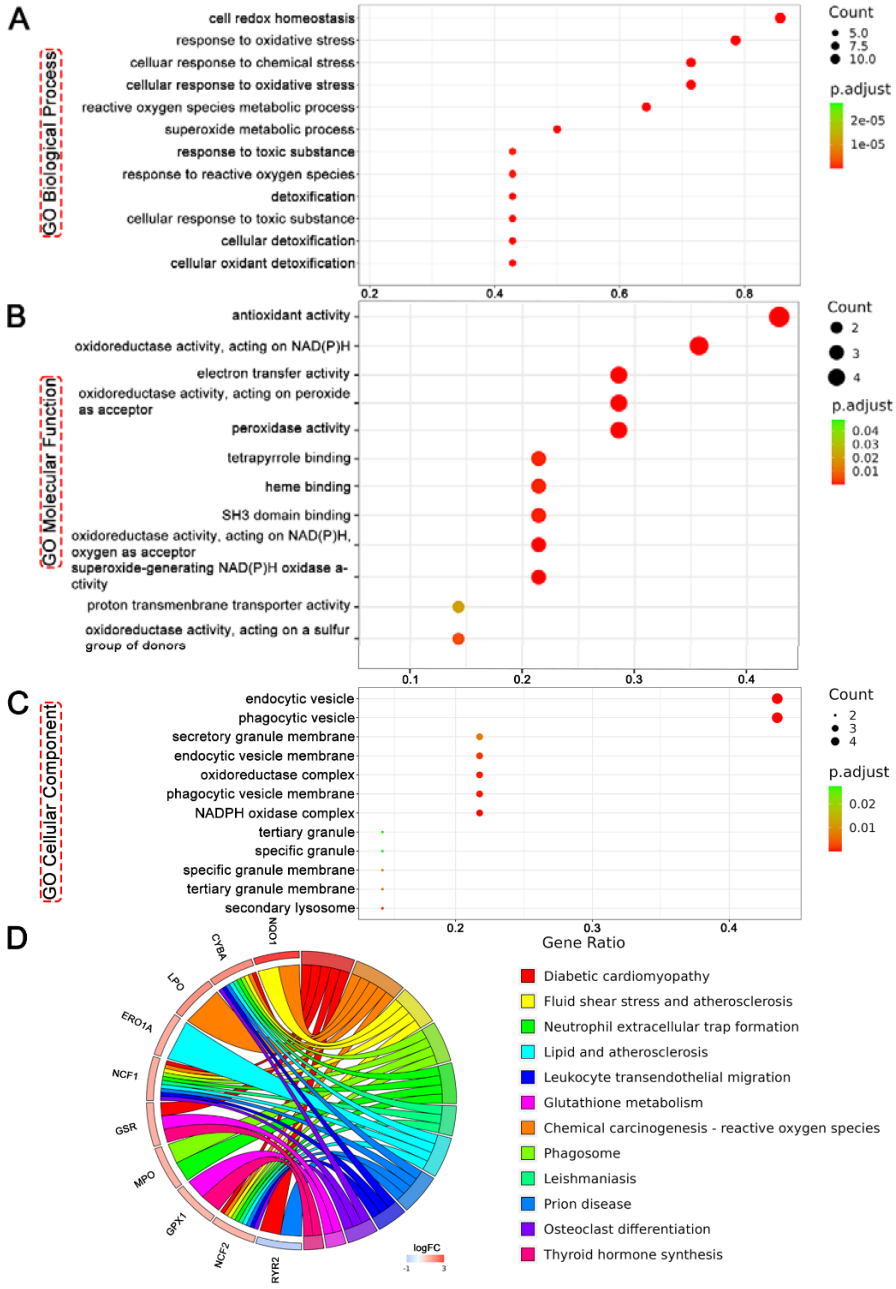

Figure 2. Functional enrichment analysis of redox-related DEGs. (A–C) The 14 redox-related DEGs of GO enrichment terms in biological process (BP), molecular function (MF) and cellular component (CC). (D) KEGG enrichment analysis.

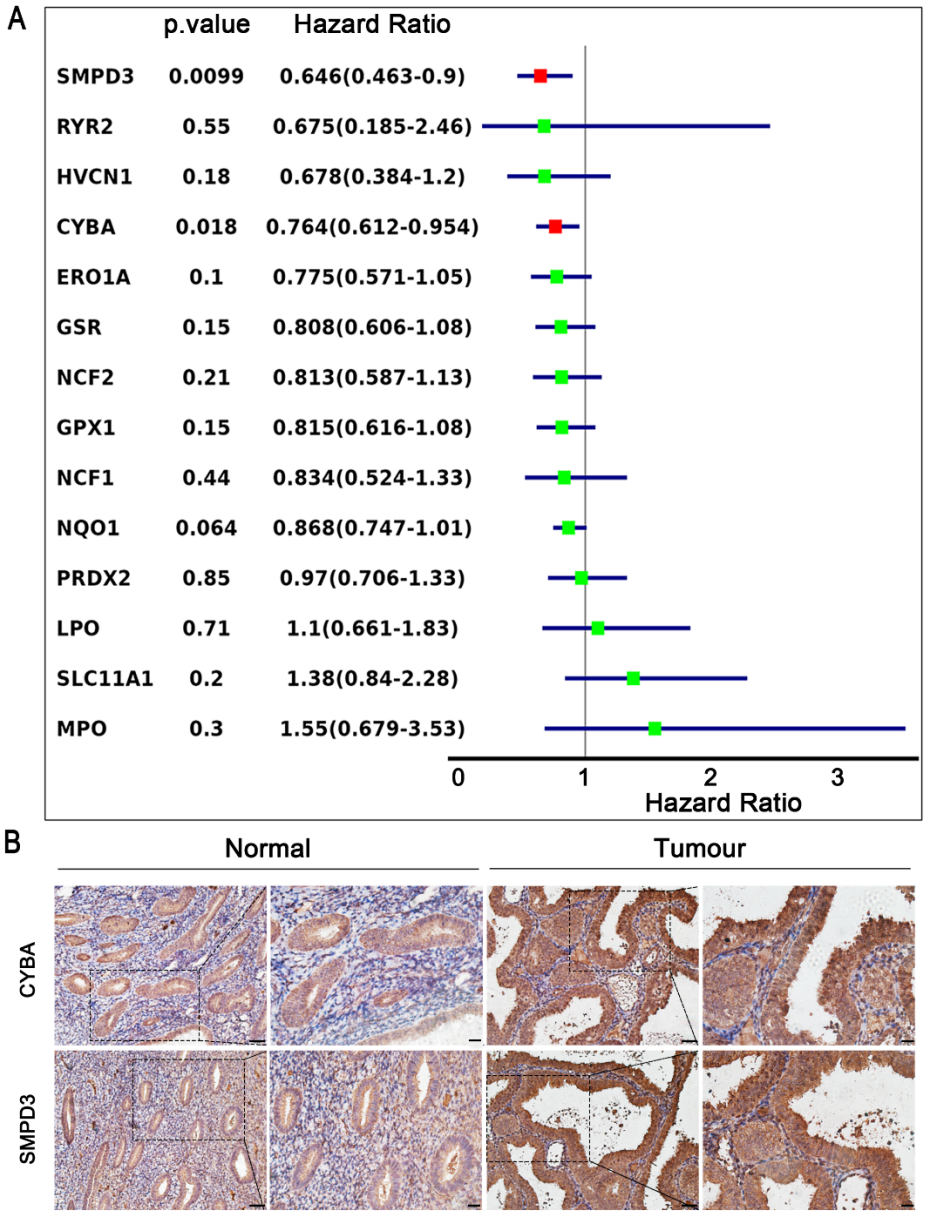

Figure 3. Construction of the risk model in the TCGA-UCEC cohort. (A) Univariate Cox regression analysis of OS for each redox-related gene. The red indicate statistical significance at $P < 0.05$ level, the green indicate no statistical significance at $P > 0.05$ level. (B) Images of IHC staining for CYBA and SMPD3 in EC tissues and paracancerous tissues. Scale bars: 20 and 50 μm.

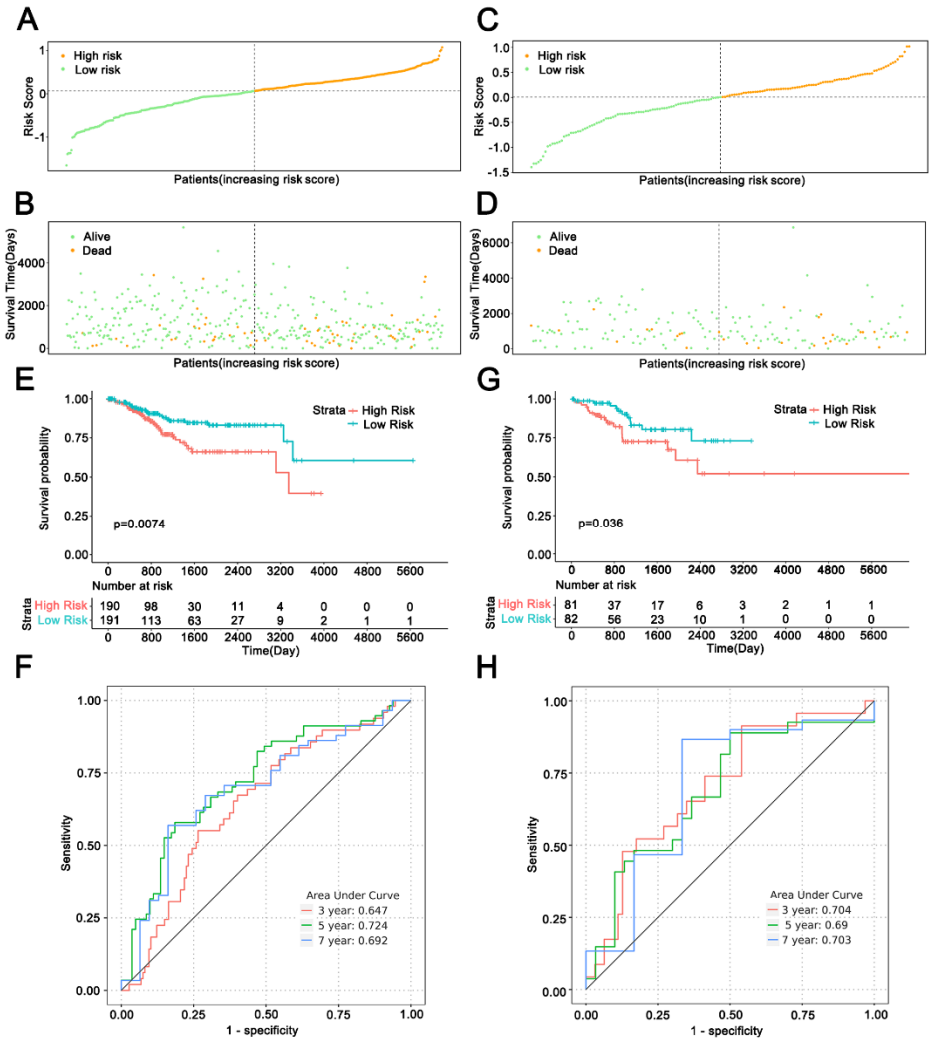

Figure 4. Validation of the risk model in the TCGA-UCEC cohort. (A, C**)** Distribution of risk scores in train sets and test sets. (B, D) The survival status of low- and high-risk EC patients in train sets and test sets. (E, G) Kaplan–Meier curves for the OS of patients in the high-and low-risk groups in train sets and test sets. (F, H) ROC curves demonstrated the predictive efficiency of the risk score in train sets and test sets.

3.4. Performance of the risk model with regard to clinical features

The risk model constructed with the two redox-related genes could effectively provide the prognosis of low-and high-risk groups with regard to different tumour stages and grades. Advanced FIGO stages had a higher risk score than early stages (Figure S3A). In addition, the risk score of the grade 3 group was higher than that of the grade 1 and 2 group (Figure S3B). These findings indicated that *CYBA* and *SMPD3* have a good ability to predict the prognosis of patients with EC with different clinical characteristics.

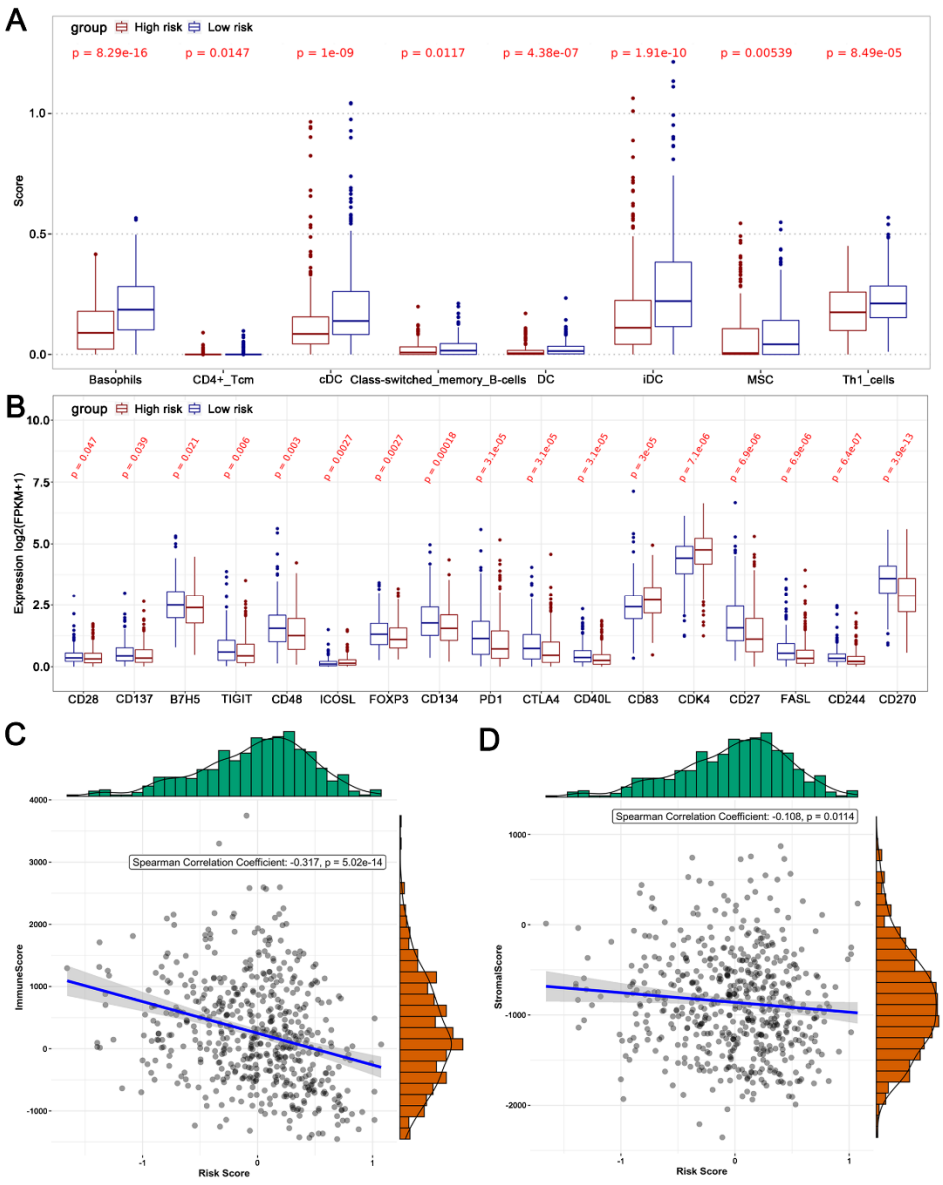

Figure 5. Comparison of immune cells and immune checkpoints in low- and high-risk groups. (A, B) Difference of immune cells and immune checkpoints between low- and high-risk groups. (C, D) Relationship between risk scores and immune and stromal scores.

3.5. GSVA

We explored the difference in the relevant pathways for both the low- and high-risk groups. The pathways were mostly enriched in 'cell cycle, RNA splicing, chromosomal region, and histone binding' in the high-risk group and 'hematopoietic cell lineage, complement activation, immunoglobulin complex and antigen binding' in the low-risk group (Figure S4A–D).

3.6. The immune microenvironment and immune checkpoints

Regarding the immune microenvironment, immune infiltration analysis revealed significantly

higher infiltration of basophils, CD4+ Tcm, cDC, class-switched memory B cells, DC, iDC, MSC, and Th1-cells in the low-risk group compared with the high-risk group ($P < 0.05$) (Figures 5A and S5A). We performed correlation analysis to determine the interaction of immune cells in immunomodulatory aspects and found a positive correlation among most immune cells (Figure S5B). We also analysed the expression of 34 immune checkpoint molecules in the high- and low-risk groups. The seventeen immune checkpoint molecules that were significantly differentially expressed between the two groups, and three molecules (ICOSL, CD83, and CDK4) presented higher expression in the high-risk group ($P < 0.05$) (Figure 5B). We calculated the stromal score and immune score by using ESTIMATE; there was a remarkable negative correlation between the tumour immune microenvironment and risk score of each patient ($P < 0.05$) (Figure 5C,D).

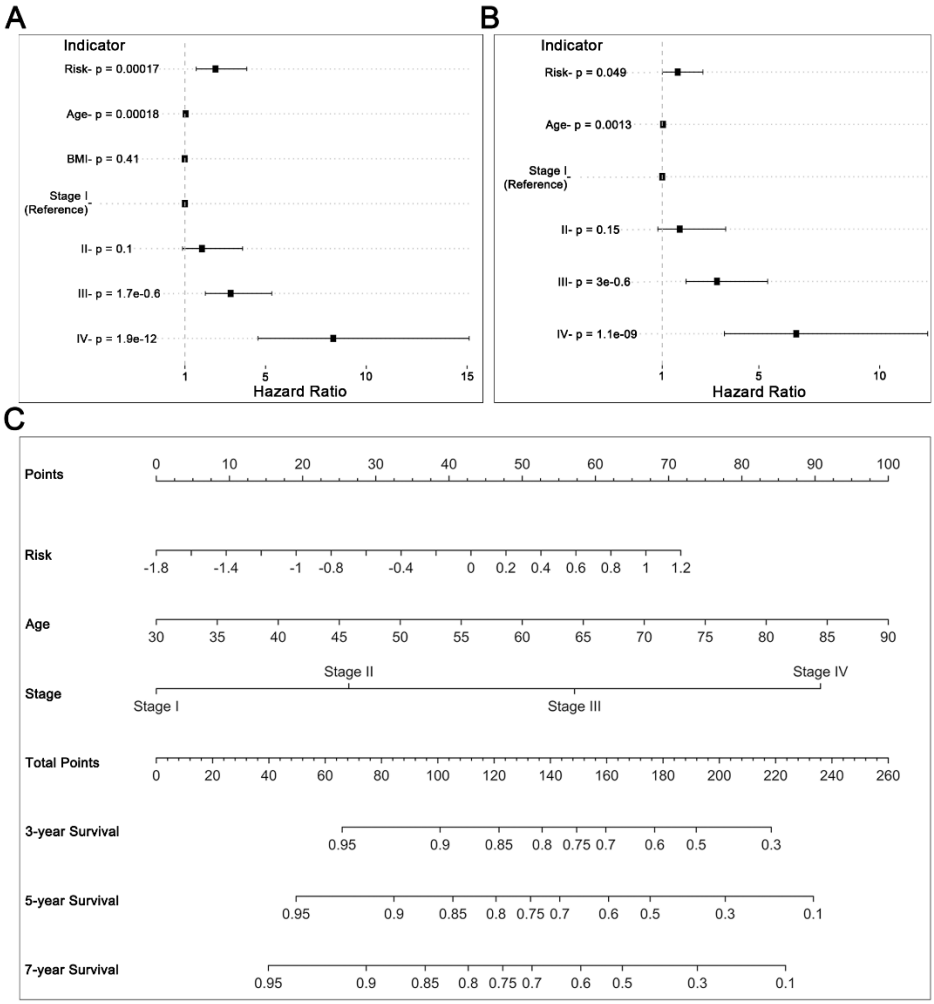

Figure 6. Construction of a nomogram. (A, B) Univariate and multivariate Cox regression analysis of the risk score and clinical characteristics. (C) Nomogram for predicting EC 3-, 5- and 7-year overall survival.

3.7. Tumour mutations in patients with EC

We filtered out the top 20 genes with somatic mutations in the low-and high-risk groups. PTEN

and TP53 had the highest mutation frequency in the low- and high-risk groups, respectively (Figure S6A,B). Then, we analysed the differences in gene mutation counts between the low- and high-risk group. The gene counts of total mutations, nonsense mutations, and missense mutations in the low-risk group was significantly higher than in the high-risk group (Figure S6C). Figure S6D shows the top 200 most frequently mutated genes in the TCGA-UCEC cohort. The three most common variant classifications in somatic mutations are missense mutation, nonsense mutation, and frame-shift-del (Figure S7A,B). The variant type in the TCGA-UCEC cohort included single nucleotide polymorphism (SNP), insertion (INS), and deletion (DEL), with SNPs being the most prevalent (Figure S7C). The C > T mutation was the most common type of somatic mutation, followed by the C > A and T > C mutations (Figure S7D). *CYBA* and *SMPD3* gene mutations occurred in 26 of the 530 samples (separately in 18 and 5 samples, respectively, and both in 3 samples) (Figure S8A). Hence, there was mainly a co-occurrence relationship among different genes in patients with EC, such as *SMPD3*, *CYBA,* and the top 20 genes with a somatic mutation (Figure S8B). The *CYBA* gene co-occurred with *PTEN*, *MUC16*, *KMT2D*, *CTCF*, *CSMD3*, *ZFHX3*, *RYR2*, *SYNE1*, *MUC5B*, *KMT2B*, *FAT4*, *ZFHX4*, *OBSCN* and *PCLO*. The *SMPD3* gene co-occurred with *PTEN*, *PIK3CA*, *TTN*, *ARID1A*, *MUC16*, *KMT2D*, *CTCF*, *CSMD3*, *ZFHX3*, *RYR2*, *SYNE1*, *MUC5B*, *KMT2B*, *FAT4*, *ZFHX4*, *OBSCN* and *PCLO*. Moreover, there was a co-occurrence relationship between *CYBA* and *SMPD3*.

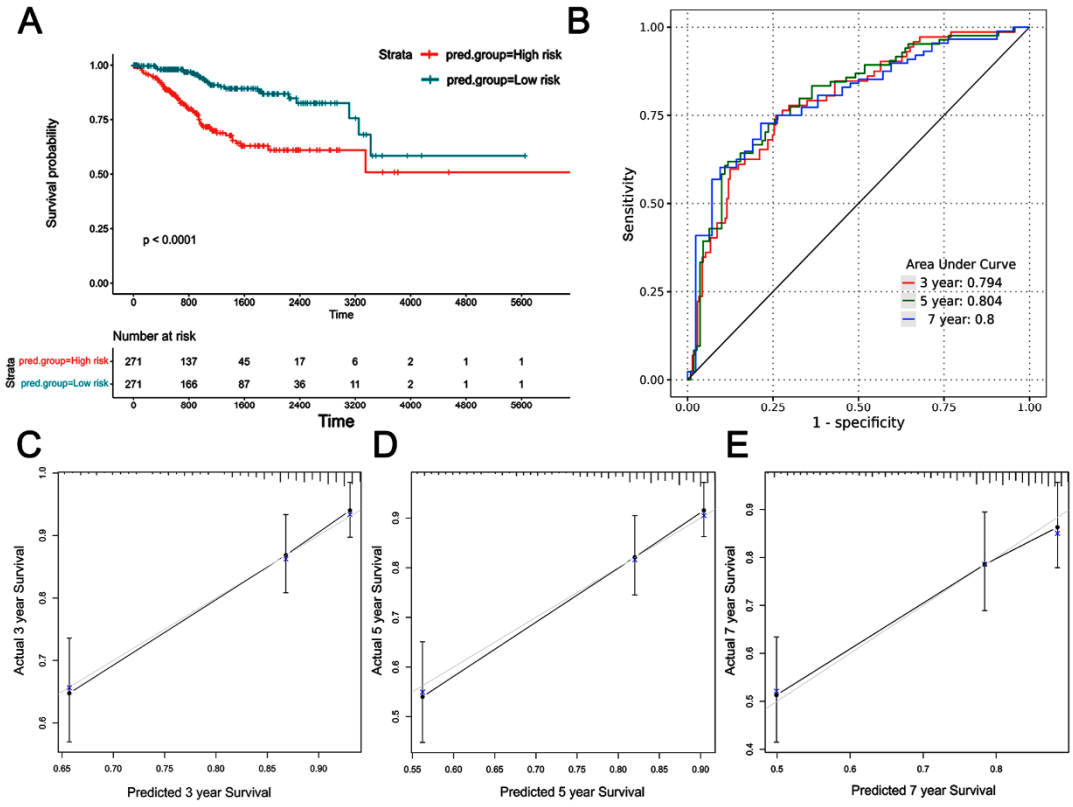

Figure 7. Evaluation of a nomogram. (A) The KM survival analysis of OS in the low- and high-risk groups. (B) The ROC curves of the nomogram with regard to 3-, 5- and 7-years survival of ECs. (C–E) The calibration curves of the nomogram.

3.8. Construction and validation of a prognostic model

We evaluated the independence of the two-gene (*CYBA* and *SMPD3*) prognostic signatures and clinical factors by univariate and multivariate Cox regression (Figure 6A,B). The risk score model and clinical features (such as clinical stage II–IV and age) were significantly correlated with prognosis. The nomogram was a quantitative model for predicting the survival probability of each patient (Figure 6C). KM survival analysis based on nomogram scores shows the OS probability of patients in the high-risk group was significantly lower than those in the low-risk group (Figure 7A). The AUC of the 3-, 5- and 7-year nomograms was 0.794, 0.804, and 0.8, respectively (Figure 7B). The calibration results indicate that the nomogram performed well (Figure 7C–E).

4. Discussion

According to global cancer statistics 2020, EC is the seventh most prevalent malignancy in the world, and the incidence of EC is growing rapidly worldwide [23]. The number of new cases with EC was 65,620 in 2020 in the United States [24]. At present, EC diagnosis and treatment are based on clinical symptoms, signs, tumour biomarkers and imaging results. The traditional treatment methods are not very effective for patients with advanced and recurrent EC. Immunotherapy is a new treatment. Although it has achieved good efficacy in the treatment of some patients with EC, there are also certain limitations, and its specific stratification effect is not clear [25]. Thus, it is necessary to find novel molecular markers in evaluating the immune responses of patients with EC to select more appropriate treatments. Redox is involved in cell differentiation, metabolism, apoptosis and proliferation of tumour cells [26–29]. Previous studies have shown oxidative stress–induced DNA damage and methylation provide growth advantages for serous EC cells by activating proto-oncogenes and silencing onco-suppressor genes, which in turn affect the occurrence and development of tumours [30–32].

In the present study, we have constructed and validated a prognostic model based on redox-related genes to predict the prognosis of patients with EC. Univariate Cox regression analysis showed that two key redox genes, namely *CYBA* and *SMPD3*, were identified as signature genes and could predict the prognosis in patients with EC. *CYBA* and *SMPD3* mRNA were overexpressed based on TCGA. We also confirmed this result in the protein expression by IHC staining. But the risk factor is < 1, this result suggested that these molecules have protective effects on patients with EC. Previous studies have shown that *CYBA* polymorphism had a protective effect on insulin resistance [33]. In addition, Montfort et.al found that SMPD3 enhances immune responses and anti-PD-1 antibody therapy in melanoma [34]. *CYBA* is a component of NADPH oxidase with CYBB [35]. Previous investigation has shown that mutation of *CYBA* is closely related to glioblastoma, familial colorectal cancer, acute myeloid leukaemia and other cancers [36–38]. *CYBA* is a specific potential immunotherapy target in patients with glioblastoma [38]. The loss of *CYBA* leads to intestinal dysfunction and further chronic bowel inflammation and colorectal cancer [36]. The increased expression of *CYBA* could also result in chemoresistance of patients with acute myeloid leukaemia [35]. *SMPD3* encodes neutral sphingomyelinase-2 (nSMase2) [39]. *SMPD3* could heighten anti-melanoma immune responses and anti-PD-1 therapy efficacy [40]. *SMPD3* has been identified as a tumour suppressor gene and an independent prognostic factor in hepatocellular carcinoma [41]. Liu et al. [42] found that *SMPD3* is also a protective prognostic gene in patients with gastric cancer. In addition, SMPD3 is also upregulation of expression in the endometrium to induce decreasing of sphingomyelin levels and

apoptosis [43]. The expression trend is the same as in EC, and it needs further research to prove whether there were differences between the two diseases. In addition, *CYBA* and *SMPD3* were previously reported to be involved in certain tumours' immune responses and metabolism signal pathways [44–47]. This result suggested that these two-redox signature genes were related to the progression of the respective cancers and the alteration of the tumour microenvironment. Although CYBA and SMPD3 have made some progress in the development of some diseases, there is little research on endothelial cells. So we hope to explore further the guiding value of *CYBA* and *SMPD3* in EC treatment and prognosis assessment. The single-cell technology and spatial transcriptomics have recently become one of the most popular experimental technology experimental technologies [48,49]. In the future, *CYBA* and *SMPD3* can be further studied in tumor genesis and clinical treatment mechanisms through single-cell technology, to promote the discovery of effective treatment targets, better guide the treatment of patients and improve their prognosis.

We used the two key redox-related genes to calculate a risk score for each sample. The regression analysis suggested that this risk model is significantly correlated with the clinical indicators and immune microenvironment of EC. It is consistent with the results of previous studies showing that a higher risk score group was positively associated with a higher clinical stage and tumour grade [50]. Some studies have shown that the number of CD4+ T cells, Th1 cells and basophils are higher than other immune cells in the tumour immune microenvironment [51–53]. T cells and dendritic cell (DC) microaggregates have been identified as excellent survival factors for patients with an immunotherapy-responsive tumour [54]. The tumour mutational burden (TMB) is often considered a marker of immunotherapy response [55]. The higher the TMB, the better the immunotherapy effect [56,57]. This study found that the total TMB in the low-risk group was higher than that in the high-risk group, suggesting that the immunotherapy effect in the low-risk group may be better than that in the high-risk group. CTLA-4, PD-1 and TIGIT are the most popular immune checkpoints [58]. In this study, the immune infiltration level; TMB; and the expression of immune checkpoints, such as CTLA-4, PD-1, and TIGIT, were higher in the low-risk group than that in the high-risk group, suggesting that the stronger the immune function, the better the immunotherapy response. Finally, we constructed a novel nomogram composed of the risk score, clinical stage and age, identified by univariate Cox and multivariate Cox regression, to quantify the probability of survival in patients with EC. The ROC and calibration curve analysis showed good predictive performance and accuracy of the nomogram for patients with EC, and the 3-, 5- and 7-year AUC was around 0.8. Hence, these two molecules can be used as biomarkers to predict the prognosis of patients with EC. Meanwhile, they could provide novel guidance for further mechanism research.

In the study, we first constructed a prognostic model based on redox genes by bioinformatics in EC. Our prognostic signature may become new prognostic biomarkers and provide potential targets for the future treatment of patients with EC. However, there are some limitations to our research. First, we only used a single database to screen redox genes and we only screened a limited number of genes. Second, our results lack a lot of experimental validation. In a future study, we will conduct experimental and clinical research.

5. Conclusions

In summary, this study based on TCGA databases identified two redox key genes, CYBA and SMPD3, which were used to construct prognostic model for the prediction of 3-, 5- and 7-year survival

probabilities in EC. In addition, the lower the risk score of this prognostic model, the better the effect of immunotherapy. The prognostic model can better predict the response to immunotherapy of patients with EC and contribute to screening out patients who were effective for immunotherapy. The redox state of cancer cells could act as an important target of precision medicine for EC. Our study provides a new direction to study tumourigenesis and development, as well as guidance for clinical diagnosis and therapy of EC. In the future, it is necessary to carry out basic research and clinical research to confirm our results.

Acknowledgments

This work was supported by research grants from the Natural Science Foundation of Hubei Province (No. 2022BCE021), the Advantages Discipline Group (Biology and Medicine) Project in Higher Education of Hubei Province (No. 2022BMXKQT2), the Natural Science Foundation of Hubei Provincial Department of Education (grant number Q20202105), the Scientific and Technological Project of Xiangyang City of Hubei Province (No. 2021YL25, 2021YL29 and 2021YL30), the "323" Public Health Project of the Hubei health commission and the Xiangyang No.1 People's Hospital (No. XYY2022-323).

Author contributions

Yan He, Han Yu and Peng Duan contributed to the conception and design of the study. The data was extracted by Nannan Cao and Yanan Tian. The data was analyzed by Yan He and Ying Zhang. Tingting Zhu and Yan He performed the collection of clinical samples and immunohistochemical. The manuscript was drafted by all authors. Han Yu and Peng Duan contributed to a critical revision and editing of the manuscript. All authors have read the manuscript, agreed the final version is ready for submission to the journal, and accepted responsibility for the manuscript's contents.

Availability of data

The datasets used in this study are freely available at TCGA-GDC portal (https://portal.gdc.cancer.gov/repository).

Conflict of interest

The authors declared no potential conflicts of interest with respect to the research, authorship, and/or publication of this article.

Ethics approval and consent to participate

The study programs complies with the ethical requirements of Helsinki Declaration and was approved by research ethics Committee of Hubei University of Medicine (Approval No. XYYYE20220029 date of approval: 05.06.2022). All patients provided written informed consent to study participation.

References

1. W. Chen, R. Zheng, P. D. Baade, S. Zhang, H. Zeng, F. Bray, et al., Cancer statistics in China, 2015, *CA: Cancer J. Clin.*, **66** (2016), 115–132. https://doi.org/10.3322/caac.21338
2. R. L. Siegel, K. D. Miller, H. E. Fuchs, A. Jemal, Cancer statistics, 2022, *CA: Cancer J. Clin.*, **71** (2021), 7–33. https://doi.org/10.3322/caac.21708
3. M. E. Urick, D. W. Bell, Clinical actionability of molecular targets in endometrial cancer, *Nat. Rev. Cancer*, **19** (2019), 510–521. https://doi.org/10.1038/s41568-019-0177-x
4. L. Mutlu, J. Harold, J. Tymon-Rosario, A. D. Santin, Immune checkpoint inhibitors for recurrent endometrial cancer, *Expert Rev. Anticancer Ther.*, **22** (2022), 249–258. https://doi.org/10.1080/14737140.2022.2044311
5. J. Ventriglia, I. Paciolla, C. Pisano, S. C. Cecere, M. Di Napoli, R. Tambaro, et al., Immunotherapy in ovarian, endometrial and cervical cancer: State of the art and future perspectives, *Cancer Treat. Rev.*, **59** (2017), 109–116. https://doi.org/10.1016/j.ctrv.2017.07.008
6. D. Xian, J. Song, L. Yang, X. Xiong, R. Lai, J. Zhong, Emerging roles of redox-mediated angiogenesis and oxidative stress in dermatoses, *Oxid. Med. Cell. Longevity*, **2019** (2019), 2304018. https://doi.org/10.1155/2019/2304018
7. H. Lan, Y. Gao, Z. Zhao, Z. Mei, F. Wang, Ferroptosis: Redox imbalance and hematological tumorigenesis, *Front. Oncol.*, **12** (2022), 834681. https://doi.org/10.3389/fonc.2022.834681
8. R. Camarda, A. Y. Zhou, R. A. Kohnz, S. Balakrishnan, C. Mahieu, B. Anderton, et al., Inhibition of fatty acid oxidation as a therapy for MYC-overexpressing triple-negative breast cancer, *Nat. Med.*, **22** (2016), 427–432. https://doi.org/10.1038/nm.4055
9. T. Poplawski, D. Pytel, J. Dziadek, I. Majsterek, Interplay between redox signaling, oxidative stress, and unfolded protein response (UPR) in pathogenesis of human diseases, *Oxid. Med. Cell. Longevity*, **2019** (2019), 6949347. https://doi.org/10.1155/2019/6949347
10. S. E. Eriksson, S. Ceder, V. J. N. Bykov, K. G. Wiman, p53 as a hub in cellular redox regulation and therapeutic target in cancer, *J. Mol. Cell Biol.*, **11** (2019), 330–341. https://doi.org/10.1093/jmcb/mjz005
11. S. K. Joseph, D. M. Booth, M. P. Young, G. Hajnóczky, Redox regulation of ER and mitochondrial Ca^{2+} signaling in cell survival and death, *Cell Calcium*, **79** (2019), 89–97. https://doi.org/10.1016/j.ceca.2019.02.006
12. E. Balta, J. Kramer, Y. Samstag, Redox regulation of the actin cytoskeleton in cell migration and adhesion: on the way to a spatiotemporal view, *Front. Cell Dev. Biol.*, **8** (2020), 618261. https://doi.org/10.3389/fcell.2020.618261
13. J. Pravda, Systemic lupus erythematosus: Pathogenesis at the functional limit of redox homeostasis, *Oxid. Med. Cell. Longevity*, **2019** (2019), 1651724. https://doi.org/10.1155/2019/1651724
14. K. Mattes, E. Vellenga, H. Schepers, Differential redox-regulation and mitochondrial dynamics in normal and leukemic hematopoietic stem cells: A potential window for leukemia therapy, *Crit. Rev. Oncol. Hematol.*, **144** (2019), 102814. https://doi.org/10.1016/j.critrevonc.2019.102814
15. A. Cruz-Gregorio, A. K. Aranda-Rivera, J. Pedraza-Chaverri, J. D. Solano, M. E. Ibarra-Rubio, Redox-sensitive signaling pathways in renal cell carcinoma, *BioFactors*, **48** (2022), 342–358. https://doi.org/10.1002/biof.1784
16. Q. Xia, X. Yang, J. L. Lu, C. Q. Liu, J. X. Sun, C. Li, et al., Development and validation of a nine-redox-related long noncoding RNA signature in renal clear cell carcinoma, *Oxid. Med. Cell. Longevity*, **2020** (2020), 6634247. https://doi.org/10.1155/2020/6634247

17. J. Ren, A. Wang, J. Liu, Q. Yuan, Identification and validation of a novel redox-related lncRNA prognostic signature in lung adenocarcinoma, *Bioengineered*, **12** (2021), 4331–4348. https://doi.org/10.1080/21655979.2021.1951522
18. K. Tu, J. Li, H. Mo, Y. Xian, Q. Xu, X. Xiao, Identification and validation of redox-immune based prognostic signature for hepatocellular carcinoma, *Int. J. Med. Sci.*, **18** (2021), 2030–2041. https://doi.org/10.7150/ijms.56289
19. Y. Wu, X. Wei, H. Feng, B. Hu, B. Liu, Y. Luan, et al., Integrated analysis to identify a redox-related prognostic signature for clear cell renal cell carcinoma, *Oxid. Med. Cell. Longevity*, **2021** (2021), 6648093. https://doi.org/10.1155/2021/6648093
20. Y. Y. Zhang, Z. J. Ni, E. Elam, F. Zhang, K. Thakur, S. Wang, et al., Juglone, a novel activator of ferroptosis, induces cell death in endometrial carcinoma Ishikawa cells, *Food Funct.*, **12** (2021), 4947–4959. https://doi.org/10.1039/D1FO00790D
21. S. Hänzelmann, R. Castelo, J. Guinney, GSVA: gene set variation analysis for microarray and RNA-seq data, *BMC Bioinf.*, **14** (2013), 7. https://doi.org/10.1186/1471-2105-14-7
22. D. Aran, Z. Hu, A. J. Butte, xCell: digitally portraying the tissue cellular heterogeneity landscape, *Genome Biol.*, **18** (2017), 220. https://doi.org/10.1186/s13059-017-1349-1
23. H. Sung, J. Ferlay, R. L. Siegel, M. Laversanne, I. Soerjomataram, A. Jemal, et al., Global cancer statistics 2020: GLOBOCAN estimates of incidence and mortality worldwide for 36 cancers in 185 countries, *CA: Cancer J. Clin.*, **71** (2021), 209–249. https://doi.org/10.3322/caac.21660
24. Y. Cai, B. Wang, W. Xu, K. Liu, Y. Gao, C. Guo, et al., Endometrial cancer: Genetic, metabolic characteristics, therapeutic strategies and nanomedicine, *Curr. Med. Chem.*, **28** (2021), 8755–8781. https://doi.org/10.2174/0929867328666210705144456
25. P. A. Ott, Y. J. Bang, D. Berton-Rigaud, E. Elez, M. J. Pishvaian, H. S. Rugo, et al., Safety and antitumor activity of pembrolizumab in advanced programmed death ligand 1-positive endometrial cancer: Results from the KEYNOTE-028 study, *J. Clin. Oncol.*, **35** (2017), 2535–2541. https://doi.org/10.1200/JCO.2017.72.5952
26. S. B. Crist, T. Nemkov, R. F. Dumpit, J. Dai, S. J. Tapscott, L. D. True, et al., Unchecked oxidative stress in skeletal muscle prevents outgrowth of disseminated tumour cells, *Nat. Cell Biol.*, **24** (2022), 538–553. https://doi.org/10.1038/s41556-022-00881-4
27. B. Jiang, J. Zhang, G. Zhao, M. Liu, J. Hu, F. Lin, et al., Filamentous GLS1 promotes ROS-induced apoptosis upon glutamine deprivation via insufficient asparagine synthesis, *Mol. Cell*, **82** (2022), 1821–1835.e6. https://doi.org/10.1016/j.molcel.2022.03.016
28. D. G. Franchina, H. Kurniawan, M. Grusdat, C. Binsfeld, L. Guerra, L. Bonetti, et al., Glutathione-dependent redox balance characterizes the distinct metabolic properties of follicular and marginal zone B cells, *Nat. Commun.*, **13** (2022), 1789. https://doi.org/10.1038/s41467-022-29426-x
29. D. W. Killilea, A. N. Killilea, Mineral requirements for mitochondrial function: A connection to redox balance and cellular differentiation, *Free Radical Biol. Med.*, **182** (2022), 182–191. https://doi.org/10.1016/j.freeradbiomed.2022.02.022
30. H. Shyam, N. Singh, S. Kaushik, R. Sharma, A. K. Balapure, Centchroman induces redox-dependent apoptosis and cell-cycle arrest in human endometrial cancer cells, *Apoptosis*, **22** (2017), 570–584. https://doi.org/10.1007/s10495-017-1346-6
31. F. Heidari, S. Rabizadeh, M. A. Mansournia, H. Mirmiranpoor, S. S. Salehi, S. Akhavan, et al., Inflammatory, oxidative stress and anti-oxidative markers in patients with endometrial carcinoma and diabetes, *Cytokine*, **120** (2019), 186–190. https://doi.org/10.1016/j.cyto.2019.05.007

32. Q. Chen, X. Zhong, X. Li, J. Wang, Research advances on the pathogenesis of endometrial serous carcinoma, *Chin. J. Obstet. Gynecol.*, **2** (2020), 142–144. https://doi.org/10.3760/cma.j.issn.0529-567X.2020.02.017
33. M. C. Ochoa, C. Razquin, G. Zalba, M. A. Martínez-González, J. A. Martínez, A. Marti, G allele of the -930A>G polymorphism of the CYBA gene is associated with insulin resistance in obese subjects, *J. Physiol. Biochem.*, **64** (2008), 127–133. https://doi.org/10.1007/bf03168240
34. A. H. Janneh, B. Ogretmen, Targeting sphingolipid metabolism as a therapeutic strategy in cancer treatment, *Cancers*, **14** (2022), 2183. https://doi.org/10.3390/cancers14092183
35. E. Tarazona-Santos, M. Machado, W. C. Magalhães, R. Chen, F. Lyon, L. Burdett, et al., Evolutionary dynamics of the human NADPH oxidase genes CYBB, CYBA, NCF2, and NCF4: functional implications, *Mol. Biol. Evol.*, **30** (2013), 2157–2167. https://doi.org/10.1093/molbev/mst119
36. L. Zhu, B. Miao, D. Dymerska, M. Kuswik, E. Bueno-Martínez, L. Sanoguera-Miralles, et al., Germline variants of CYBA and TRPM4 predispose to familial colorectal cancer, *Cancers*, **14** (2022), 670. https://doi.org/10.3390/cancers14030670
37. R. Paolillo, M. Boulanger, P. Gâtel, L. Gabellier, M. De Toledo, D. Tempé, et al., The NADPH oxidase NOX2 is a marker of adverse prognosis involved in chemoresistance of acute myeloid leukemias, *Haematologica*, **107** (2022). https://doi.org/10.3324/haematol.2021.279889
38. M. Rose, T. Cardon, S. Aboulouard, N. Hajjaji, F. Kobeissy, M. Duhamel, et al., Surfaceome proteomic of glioblastoma revealed potential targets for immunotherapy, *Front. Immunol.*, **12** (2021), 746168. https://doi.org/10.3389/fimmu.2021.746168
39. J. Wang, J. Li, J. Gu, J. Yu, S. Guo, Y. Zhu, et al., Abnormal methylation status of FBXW10 and SMPD3, and associations with clinical characteristics in clear cell renal cell carcinoma, *Oncol. Lett.*, **10** (2015), 3073–3080. https://doi.org/10.3892/ol.2015.3707
40. A. Montfort, F. Bertrand, J. Rochotte, J. Gilhodes, T. Filleron, J. Milhès, et al., Neutral sphingomyelinase 2 heightens anti-melanoma immune responses and Anti-PD-1 therapy efficacy, *Cancer Immunol. Res.*, **9** (2021), 568–582. https://doi.org/10.1158/2326-6066.CIR-20-0342
41. K. Revill, T. Wang, A. Lachenmayer, K. Kojima, A. Harrington, J. Li, et al., Genome-wide methylation analysis and epigenetic unmasking identify tumor suppressor genes in hepatocellular carcinoma, *Gastroenterology*, **145** (2013), 1424–1435. https://doi.org/10.1053/j.gastro.2013.08.055
42. X. Liu, J. Wu, D. Zhang, Z. Bing, J. Tian, M. Ni, et al., Identification of potential key genes associated with the pathogenesis and prognosis of gastric cancer based on integrated bioinformatics analysis, *Front. Genet.*, **9** (2018), 265. https://doi.org/10.3389/fgene.2018.00265
43. Y. H. Lee, C. W. Tan, A. Venkatratnam, C. S. Tan, L. Cui, S. F. Loh, et al., Dysregulated sphingolipid metabolism in endometriosis, *J. Clin. Endocrinol. Metab.*, **99** (2014), E1913–1921. https://doi.org/10.1210/jc.2014-1340
44. C. Zhang, Z. Li, F. Qi, X. Hu, J. Luo, Exploration of the relationships between tumor mutation burden with immune infiltrates in clear cell renal cell carcinoma, *Ann. Transl. Med.*, **7** (2019), 648. https://doi.org/10.21037/atm.2019.10.84
45. J. Lu, P. Wilfred, D. Korbie, M. Trau, Regulation of canonical oncogenic signaling pathways in cancer via DNA methylation, *Cancers*, **12** (2020), 3199. https://doi.org/10.3390/cancers12113199
46. Y. Shen, M. Takahashi, H. M. Byun, A. Link, N. Sharma, F. Balaguer, et al., Boswellic acid induces epigenetic alterations by modulating DNA methylation in colorectal cancer cells, *Cancer Biol. Ther.*, **13** (2012), 542–552. https://doi.org/10.4161/cbt.19604

47. K. Revill, T. Wang, A. Lachenmayer, K. Kojima, A. Harrington, J. Li, et al., Genome-wide methylation analysis and epigenetic unmasking identify tumor suppressor genes in hepatocellular carcinoma, *Gastroenterology*, **145** (2013), 1424–1435.e25. https://doi.org/10.1053/j.gastro.2013.08.055
48. Q. Song, X. Zhu, L. Jin, M. Chen, W. Zhang, J. Su, SMGR: a joint statistical method for integrative analysis of single-cell multi-omics data, *NAR Genomics Bioinf.*, **4** (2022), lqac056. https://doi.org/10.1093/nargab/lqac056
49. Z. Tang, T. Zhang, B. Yang, J. Su, Q. Song, spaCI: deciphering spatial cellular communications through adaptive graph model, *Briefings Bioinf.*, **24** (2023), bbac563.50. https://doi.org/10.1093/bib/bbac563
50. M. Zheng, Y. Hu, R. Gou, S. Li, X. Nie, X. Li, et al., Development of a seven-gene tumor immune microenvironment prognostic signature for high-risk grade III endometrial cancer, *Mol. Ther. Oncolytics*, **22** (2021), 294–306. https://doi.org/10.1016/j.omto.2021.07.002
51. Y. Fan, X. Li, L. Tian, J. Wang, Identification of a metabolism-related signature for the prediction of survival in endometrial cancer patients, *Front. Oncol.*, **11** (2021), 630905. https://doi.org/10.3389/fonc.2021.630905
52. S. Singh, X. H. F. Zhang, J. M. Rosen, TIME is a great healer-targeting myeloid cells in the tumor immune microenvironment to improve triple-negative breast cancer outcomes, *Cells*, **10** (2020), 11. https://doi.org/10.3390/cells10010011
53. I. Mito, H. Takahashi, R. Kawabata-Iwakawa, S. Ida, H. Tada, K. Chikamatsu, Comprehensive analysis of immune cell enrichment in the tumor microenvironment of head and neck squamous cell carcinoma, *Sci. Rep.*, **11** (2021), 16134. https://doi.org/10.1038/s41598-021-95718-9
54. Z. Abdulrahman, S. J. Santegoets, G. Sturm, P. Charoentong, M. E. Ijsselsteijn, A. Somarakis, et al., Tumor-specific T cells support chemokine-driven spatial organization of intratumoral immune microaggregates needed for long survival, *J. ImmunoTher. Cancer*, **10** (2022), e004346. http://dx.doi.org/10.1136/jitc-2021-004346
55. C. F. Friedman, J. D. Hainsworth, R. Kurzrock, D. R. Spigel, H. A. Burris, C. J. Sweeney, et al., Atezolizumab treatment of tumors with high tumor mutational burden from mypathway, a multicenter, open-label, phase IIa multiple basket study, *Cancer Discov.*, **12** (2022), 654–669. https://doi.org/10.1158/2159-8290.CD-21-0450
56. M. J. Riggs, N. Lin, C. Wang, D. W. Piecoro, R. W. Miller, O. A. Hampton, et al., DACH1 mutation frequency in endometrial cancer is associated with high tumor mutation burden, *PLoS One*, **15** (2020), e0244558. https://doi.org/10.1371/journal.pone.0244558
57. Y. Zhang, J. Zhang, Z. Shao, L. Zhao, Y. Zhang, S. Zhang, et al., Mutational landscapes and tumour mutational burden expression in endometrial cancer, *Ann. Onco.*, **30** (2019), v424–v425. https://doi.org/10.1093/annonc/mdz250.048
58. M. Collin, Immune checkpoint inhibitors: a patent review (2010–2015), *Expert Opin. Ther. Pat.*, **26** (2016), 555–564. https://doi.org/10.1080/13543776.2016.1176150